A PRELIMINARY ANALYSIS OF THE RHEOLOGICAL TRANSFORMATION DUE TO WATER INFILTRATION AS A MECHANISM FOR HIGH MOBILITY OF SUBMARINE MASS MOVEMENTS

Sueng Won JEONG, Université Laval, Québec, Canada
Jacques LOCAT, Université Laval, Québec, Canada
Serge LEROUEIL, Université Laval, Québec, Canada

ABSTRACT

This study describes one of the main issues of the COSTA-Canada (Continental Slope Stability, www.costa-canada.ggl.ulaval.ca) project. It aims at contributing to the understanding of transition mechanisms. As for the transformation of a soil under water during shearing, water infiltration into soils could influence the transformation of the debris and influence the mobility. In the light of water infiltration into soils, the laboratory vane test was conducted. Recently, this study has focused more on the rheological transformation from failure to post-failure. In a sense, this is also related to previous field work data and viscometric data. The final goal of this study is to determine the rheological transformation and increase in mobility of submarine mass movement due to water infiltration. From these points of view, the strength parameter for remoulded materials due to an increase in water content will be discussed in terms of a linear log-log relationship between shear stress (τ) and strain rate (γ). At a consequence, the normalized strength parameter ($\Delta\tau/\tau$) per log cycle of strain rate is about 34% for all materials.

RÉSUMÉ

Cette étude décrit un élément du projet COSTA-Canada (stabilité des pentes continentales, www.costa-canada.ggl.ulaval.ca). Elle vise contribuerées la compréhension des mécanismes de transition lorsque la masse passe de la rupture à l'étape de post-rupture. Au moment de la transformation des sols sous-marins lors d'un cisaillement, l'infiltration d'eau peut influencer cette transformation ainsi que la mobilité des débris engendrés. Afin d'éclaircir le rôle que joue l'eau infiltrée, des essais au scissomètre ont été réalisés en laboratoire. Récemment, cette étude a porté davantage sur l'aspect hydrodynamique du déclenchement du glissement. Les objectifs sont de coupler l'interaction sol-eau pour voir l'influence du mouvement de l'eau autour de la masse en mouvement et d'évaluer son rôle potentiel sur la transformation des débris et la mobilité associée. Suite à cette étude, la variation du résistance du sol remanié, associée à une augmentation de la teneur en eau dans le matériel remanié et sera examinée par une relation log-log entre la contrainte de cisaillement (τ) et la vitesse de cisaillement (γ). Le paramètre résistance normalisé résultant ($\Delta\tau/\tau$) est approximativement de 34% pour cent pour cycle logarithmique pour tous les matériaux.

1. INTRODUCTION

It has been postulated by Locat and Lee (2002) that there has to be ways of increasing the water content of a remoulded soils in order to achieve the low strength required to provide some of the highly mobile subaqueous mass movements. For example, high volume of sediments have been displaced in excess of several hundreds kilometers, i.e., the Mississippi Fan (Locat et al., 1996). It is also believed (Locat and Lee, 2002) that this phenomenon can occur during the transitions from failure to post-failure, i.e., from the slide initiation to its transformation into a flowing materials (Fig. 1). This is illustrated in Fig. 1 which shows 4 stages of slope movements: 1 - prefailure; 2 - failure; 3 - post-failure associated with the transformation; 4 - flow. As shown in Fig. 1, in this study we have focused more on the evolution from remoulded shear strength (C_{ur} in stage 3) to flowing one (τ_c in stage 4) under undrained conditions. This transition builds on interaction between sediment and water in that it considers on changes in geomechanical properties of submerged soils due to water infiltration. It is assumed that the water content and density remain unchanged until an ambient water surrounding sliding mass helps to break into many pieces of soils, and subsequently reduce the cohesion or shear strength (e.g., stage 4 in Fig. 1). Consequently, during this process, the overall water content in materials will gradually increase, and the density will decrease, until it becomes a flowing material with flow-like characteristics. In the course of this evolution of strength, the transformations will depend on the nature of the materials involved, sensitivity, interaction between particles, degree of consolidation (Locat et al., 1996), energy transformation, and so on. The final objective is to examine the rheological transformation caused by soil-water interaction on its potential role in transforming the debris or influencing their mobility. As for the point T in Fig. 1, the followings are considered: (1) strain rate dependent on soil behaviour; (2) rheological analysis related to the strength parameter.

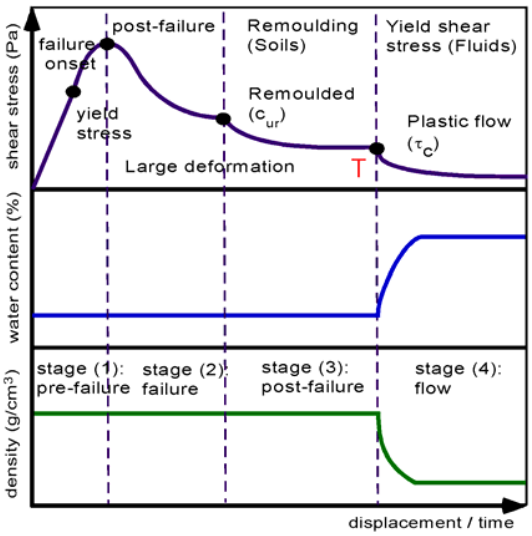

Fig. 1 Schematic view of strength evolution with displacement (or time)

1.1 Strain rate dependency of soil behavior

It is generally recognized that an increase in the rate of shear strain results in an increase in undrained shear strength. The variation of the strength parameter, $\Delta C_u/C_u$, is typically of 10 ~ 15% per log cycle of rate when inorganic intact clays are considered (Leroueil and Marques, 1996). From the results considered by these authors, the strength was typically reached at strain rates between 10^{-7} and 10^{-5} (s^{-1}). They also showed that the preconsolidation pressure and axial strain rate can generally be related by a straight line in a log–log diagram. In general, for inorganic intact clays:

$$\frac{\Delta C_u}{C_u} \approx \frac{\Delta \sigma'_p}{\sigma'_p} = 0.1 \cdot \Delta \log(\dot{\varepsilon}_1) \qquad [1]$$

where, C_u and σ'_p are the undrained shear strength and preconsolidation pressure, respectively; $\dot{\varepsilon}_1$ is the axial strain rate.

From a rheological point of view, the shear stress and strain rate can be described as a linear relation in a log τ – log γ diagram in Eqs. 2 and 3:

$$\log \tau = A \cdot \log \gamma + B \qquad [2]$$

$$\log\left(\frac{\tau}{\tau_o}\right) = A \cdot \log\left(\frac{\gamma}{\gamma_o}\right) \qquad [3]$$

where, τ_o is shear stress corresponding to the reference strain rate (γ_o). *A* and *B* are soil dependent parameters. These parameters will be discussed herein later. From the rheological perspective, this strength parameter *A* will be considered for rheologcial transformation in relation with the variation of strength due to an increase in water content.

1.2 Rheological models

Rheology is known as the science of the deformation and flow of matter, and the emphasis on flow means that it is concerned with the relationship between shear stress (τ, Pa) and strain rate (γ, s^{-1}), sometimes referred to as a rheogram. The simplest theoretical model that associates fluids to a yield stress is well known as a Bingham model. However Bingham model can not be fitted to flow curves in the whole range of shear rates. A more complex situation, of great interest within the context of this study, is encountered with materials with flow curves being in agreement with the following equations (Coussot, 1997; Locat 1997; Imran et al. 2001):

Bingham:

$$\tau = \tau_c + \eta \cdot \gamma \qquad [4]$$

Herschel-Bulkley:

$$\tau = \tau_c + K \cdot \gamma^n \qquad [5]$$

Power law:

$$\tau = K \cdot \gamma^n \qquad [6]$$

Casson:

$$\sqrt{\tau} = \sqrt{\tau_c} + \sqrt{K\gamma} \qquad [7]$$

Bilinear:

$$\tau = \tau_{ya} + \eta_{pl} \cdot \gamma^n + \left(\frac{\tau_c \cdot \gamma_o}{\gamma + \gamma_o}\right) \qquad [8]$$

where τ is the shear stress (Pa), τ_c is the yield stress (Pa), τ_{ya} is the apparent yield stress (Pa), and γ is the shear rate (s^{-1}). *K* is the consistency coefficient (Pa.s), and exponent '*n*' is the flow behaviour index (dimensionless). In Eq. 6, if *n* = 1, the power law equation simplifies to the Newtonian model. The bilinear model (Eq. 8) suggested by Locat (1997) and Imran et al. (2001), where γ_o is the shear rate at the yield stress or a rheological constant with unit of shear rate. The plastic viscosity (η_{pl}) of the first part of the bilinear model is given by the ratio τ_o/γ_o (Locat, 1997; Imran et al., 2001). It approaches a Bingham fluid behaves as the exponent *n* get closer 1. Figure 2 shows the different models fitted with experimental data of the leached Jonquière clays. In most cases the best-fit is given with a bilinear model.

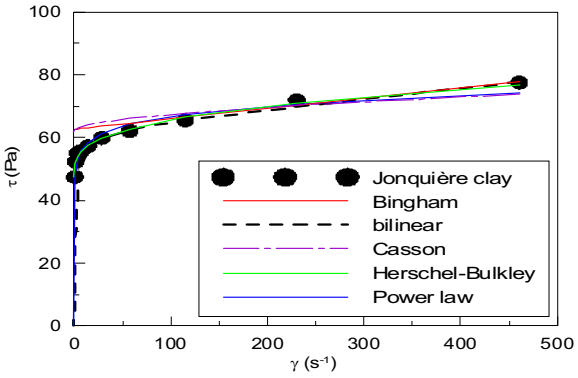

Fig. 2 Comparison of different rheological models with experimental data on Jonquière clay

On the basis of these hypotheses (Fig. 1), the methodologies are linked to the laboratory vane tests and rheological analyses in the following sections.

2. MATERIALS AND METHODS

The rheological transformations associated with submarine mass movements will be examined using the laboratory vane tests and viscometric data. In order to identify the interaction between submarine sediments and ambient water (or effects of water infiltration from stage 3 to stage 4) based on the hypotheses given in Fig. 1, a series of laboratory vane tests were conducted. As shown in Table 1, the 7 tests for Saguenay fjord were conducted, and the vane blades used had diameter and height of 12.7 mm × 12 mm or 12.7 mm × 21.0 mm. In these tests, the values of strengths cannot taken into account because of unreliable calibration of the vane springs. The samples were subjected to the following conditions: (1) a measurement of intact and remoulded shear strength with different vane blades; (2) testing at submerged conditions; (3) a waiting period of 24 hours after a measurement of remoulded shear strength.

Secondly, as to the rheological analysis, most of the samples are soft clays in the data published by Locat (1997) and obtained from other tests in Fig. 4, except for some samples, i.e., BEAU and la Valette soils (Locat, 1997). All the rheological tests were carried out with the Rotovisco RV-12, which is run in a steady state regime. The detailed procedures followed for viscometric measurements are described in Locat and Demers (1988) and Perret et al. (1996). These procedures may include three types of tests: (1) constant shear rate; (2) dynamic response; and (3) hysteresis. The rheological assessment of the known rheological models, i.e., Bingham plastic, Herschel-Bulkley, bilinear and log-log approach, will be examined in relation with soil type, salinity, and liquidity index to represent sediment concentration (Locat, 1997). As introduced before, the strength parameter *A* (Eq. 3) using a normalized log-log diagram is also discussed.

3. RESULTS AND ANALYSIS

3.1 Experimental evidence related to transformation using laboratory vane

In Fig. 3, the evolution of strengths with vane rotation and the change in water content before and after saturation are shown. The vertical dashed line is the boundary between the natural and the condition with increased water content. The measurement of water content is given only for the central point where the vane blade penetrated. In the stage (3) of Fig. 3, at the vane rotation of 200 (°), under submerged soil conditions, the results show a significant gradual decrease in undrained shear strength associated with the increases in water content. If our hypothesis in Fig. 1 is correct, that means that the water infiltration during shearing helps to reduce the undrained shear strength. Table 1 shows the results for Saguenay fjord (Bras Nord, Baie des Ha! Ha! and Pointe-du-Fort), the materials used are soft clays except for Baie des Ha! Ha!. The change in strength and water content for the Pointe-du-Fort sample is much more significant than the Baie des Ha! Ha!.

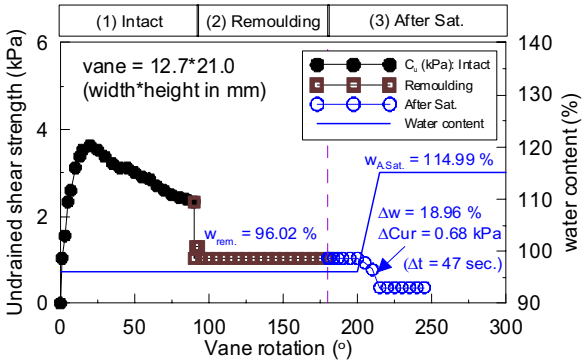

Fig. 3 Results of laboratory vane tests (Bras Nord of Saguenay fjord, depth = 160 cm)

3.2 Rheological properties in pseudo-plastic regimes

From the viscometric results, Figure 4a, b, c & d show the empirical relationships for: (1) the yield stress and viscosity; (2) liquidity index and viscosity; (3) liquidity index and yield stress and (4) liquidity index and Newtonian viscosity (η_l). Even if the scatter is important, results are closed to the empirical relationships proposed by Locat (1997) and are much better for a given soils. As for the silty soils (*i.e.*, IOC in Fig. 4), the plastic viscosity only represents about 1/1000 of the total shearing resistance of the sediments. Additionally, Fig. 4.d shows that the relationship between the liquidity index and Newtonian viscosity (η_l) for the bilinear model. This relationship shows a similar trend with others.

Table 1. Summary of laboratory vane tests

No.	Sample	Depth (m)	Description	w_n (%)	Sat.(hours)	P (cm)	Δw (%)	ΔI_L
1	COR0210-STA-13 (Pointe-du-Fort)	5.4	Soft Clay	84.1	24	4.5 cm	10.26	0.24
2	COR0210-STA-13 (Pointe-du-Fort)	5.7	Soft Clay	86.1	24	4.5 cm	6.19	0.14
3	MD992223 (Baie des Ha ! Ha !)	26.85	Silty clay	39.9	24	Surface	1.57	0.05
4	MD992223 (Baie des Ha ! Ha !)	19.65	Sandy silty clay	31.0	3	Surface	2.11	0.12
5	MD992223 (Baie des Ha ! Ha !)	19.65	Sandy silty clay	31.0	24	≅ 4.0 cm	2.29	0.12
6	BRAS NORD	1.60-1.75	Soft Clay	96.4	0	Surface	5.36	0.10
7	BRAS NORD	1.60-1.75	Soft Clay	96.0	24	Surface	18.96	0.34

NOTE: w_n = natural water content; P (cm) = penetration depth of vane blade; Sat. (hours) = saturation; ΔI_L = variation in liquidity index, and Δw = variation in water content.

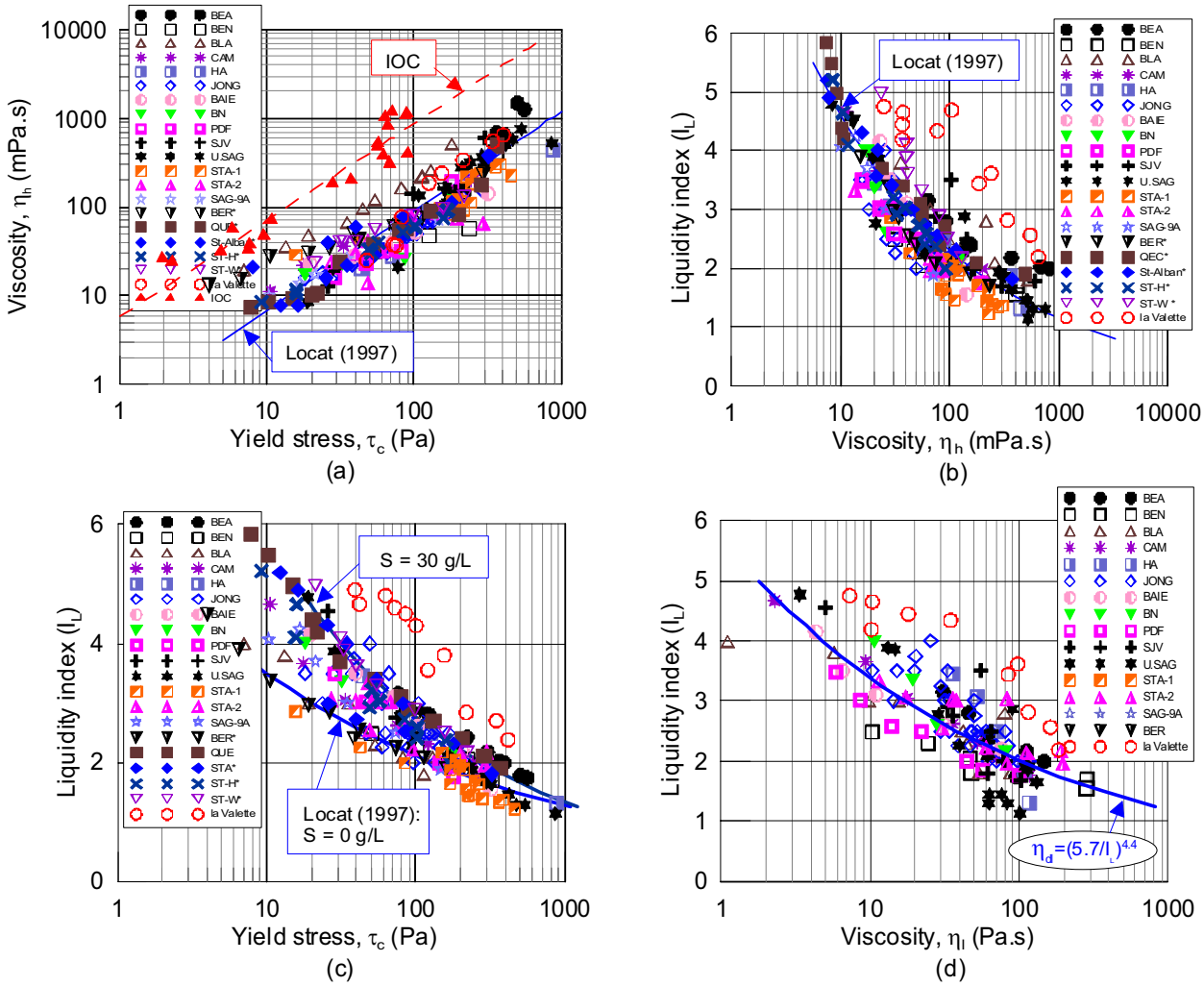

Fig. 4 Rheological relationships among the yield stress, viscosity, and liquidity index (I_L). Note that viscosity η_l and η_h are Newtonian and Bingham viscosity, respectively. (BEA: Beaufort; BEN: Bentonite; CAM: Cambridge; HA: Hudson Apron; JONQ: Jonquière; BAIE: Baie des Ha! Ha!; BN: Bras Nord; PDF: Pointe-du-Fort; SJV: Sainte-Jean-Vianney; U.SAG: Upper Saguenay area; BER: Berthierville; QUE: Québec; ST-H: St-Hyacinthe; ST-W : St-Wenceslas; STA: St-Alban)

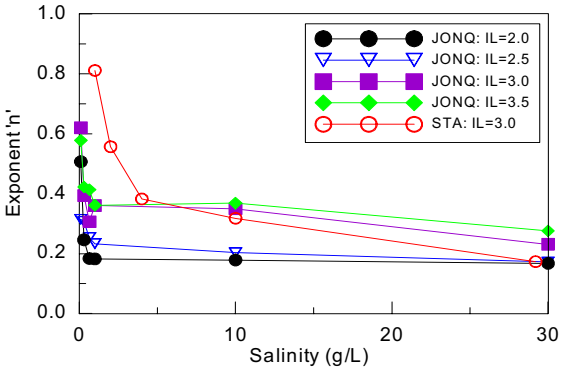

Fig. 5 Relationship between salinity (in g/L) and exponent '*n*' using Herschel-Bulkley model (modified from Locat (1997))

The relationship between the salinity (in g/L) and exponent *n* for Jonquière and St-Alban clays are shown in Fig. 5. At a high salinity (*i.e.*, 30 g/L), the flow behaviours are typical of pseudo-plastic fluid, *i.e.,* the viscosity tends to gradually decrease with increasing shear rate. On the other hand, at high water content and at low salinity the behaviour gets closer to that of a Bingham fluid, the value of *n* tending towards 1.0. The comparison of yield stress determined by Bingham model and remolded shear strength measured by Swedish fall cone is plotted in Figure 6. The ratio of τ_c / C_{ur} is about 0.8.

In order to identify the most appropriate models for given data and test results, the Jonquière and St-Ablan clays were selected. These clays have clay fractions (≤2 μm) of about 60 % and 46 %, respectively. The main physico-chemical properties of these soils are gathered in Table 2. All tests in Table 3 are conducted using the Sensor MV-II. As shown in Table 3, the different models were applied to find the compatible rheological model considering variations in salinity and in water content. Coefficient of determination r^2 shows how well the data are explained by the best-fit line. Most of the rheological models have a good results, for examples, $r^2 \geq 0.9$, except for Bingham model. However, Bingham model tends to be better with increasing water content, most likely for the reasons mentioned above.

Table 2. Physico-chemical identification of the Jonquière and St-Alban clays

	w_L (%)	w_p (%)	I_p (%)	S.S	S
Jonquière	52	22	30	65	0.1
St-Alban	36	19	17	52	0.3

Note: w_L = liquid limit; w_p = plastic limit; I_p = plasticity index; S.S = Specific area (m^2/g) and S = salinity (g/L). (from Perret et al. (1996) and Locat (1997))

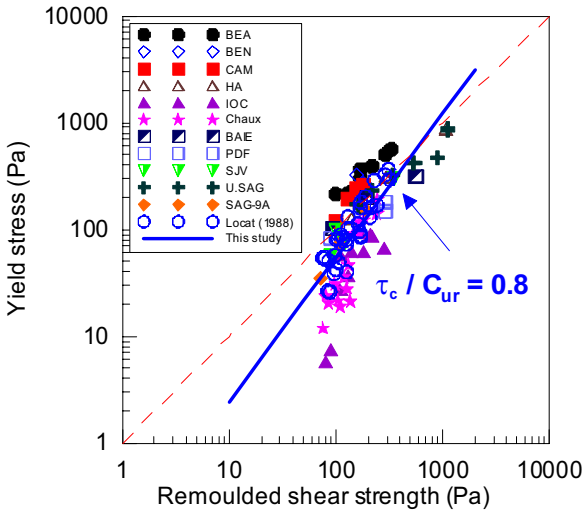

Fig. 6 Relationship between yield stress and remoulded shear strength

3.3 Rheological transformations in terms of strength parameter

Fig. 7 is one of the examples for the relationships between shear stress and strain rate on Jonquière clays at a constant liquidity index of 2.5. Fig. 7b, 7c and 7d show the linear log-log relations with different scale of shear stress (τ). As shown in Fig. 7.c and 7.d, the relationship between shear stress and strain rate can be expressed in terms of log (τ) – log (γ) scale (See Eq. 2). Based on these relationships, the normalized strength parameter *A* in log-log relations (e.g., Figs. 7.d) can be obtained for various liquidity indices and salinity. The applied strain rates in tests are shown from 1 to 10^3 (s^{-1}). Totally, the normalized strength parameters *A* are shown as roughly 0.05 ~ 0.12 in log-log relations. As for new log-log approach between shear stress (τ) and strain rate (γ), the normalized strength parameters *A* in all tests are shown as roughly 0.1 ~ 0.4, corresponding to about 34 % in log-log relations.

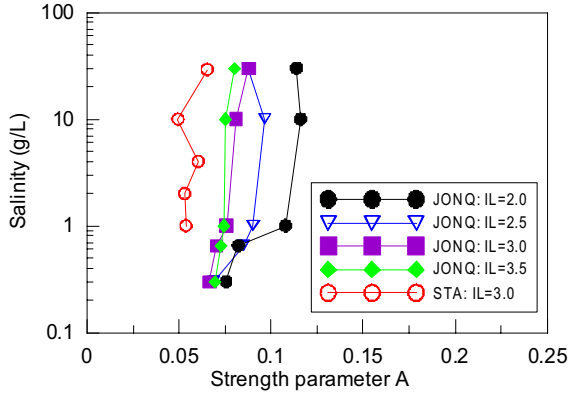

Fig. 8 Relationship between salinity (g/L) and *A* values

Table 3. Rheological parameters for Jonquière and St-Alban clays (data from Martignoni, 1991; Locat, 1997)

	Model		Bingham			Herschel-Bulkley				bilinear			Log-log		
	I_L	S	τ_c_B	η_h_B	r^2	τ_c_HB	*K*_HB	*n*_HB	r^2_HB	τ_c_bi	η_l_bi	r^2_bi	A	B	r^2
	2.00	0.10	95.1	49.89	0.983	74.0	15.4	0.13	0.954	96.0	61.91	0.993	0.033	4.48	0.747
	2.00	0.30	132.5	68.31	0.751	92.9	15.0	0.25	0.997	133.0	69.43	0.983	0.076	4.60	0.955
	2.00	0.65	217.7	113.77	0.693	137.6	39.2	0.18	0.965	218.0	112.80	0.960	0.082	5.07	0.878
	2.00	1.00	216.0	121.00	0.608	112.8	50.6	0.18	0.964	217.0	97.09	0.985	0.108	4.95	0.856
	2.00	10.00	199.3	111.44	0.592	96.6	50.4	0.18	0.953	201.0	85.81	0.984	0.116	4.83	0.838
	2.00	30.00	288.2	153.64	0.591	155.3	69.2	0.17	0.999	290.0	116.89	0.982	0.114	5.21	0.892
	2.50	0.10	45.8	26.58	0.945	30.0	9.9	0.15	0.871	46.0	29.66	0.988	0.049	3.69	0.794
	2.50	0.30	62.6	33.34	0.819	47.4	4.4	0.31	0.983	63.0	33.76	0.974	0.069	3.88	0.960
	2.50	0.65	96.4	54.79	0.750	64.7	11.6	0.25	0.995	97.0	48.80	0.983	0.085	4.25	0.959
	2.50	1.00	105.3	62.95	0.734	67.3	15.2	0.23	0.995	106.0	52.39	0.984	0.090	4.32	0.942
	2.25	10.00	104.9	59.68	0.711	63.9	15.8	0.24	0.958	105.0	84.14	0.973	0.097	4.28	0.946
JONQ	2.50	30.00	166.4	81.36	0.698	59.0	20.6	0.17	0.949	104.0	79.96	0.946	0.088	4.77	0.968
	3.00	0.10	23.5	17.95	0.934	15.0	4.9	0.16	0.791	24.0	14.37	0.937	0.057	2.98	0.708
	3.00	0.30	47.5	25.23	0.854	37.7	1.9	0.39	0.976	48.	33.76	0.958	0.067	3.61	0.956
	3.00	0.65	58.6	31.62	0.824	44.1	4.2	0.31	0.997	59.0	31.68	0.971	0.071	3.81	0.961
	3.00	1.00	59.0	34.03	0.831	44.7	3.2	0.36	0.997	60.0	31.00	0.966	0.076	3.80	0.977
	3.25	10.00	58.8	31.47	0.789	42.1	3.8	0.35	0.975	59.5	29.75	0.967	0.081	3.76	0.986
	3.00	30.00	103.2	48.73	0.707	43.9	8.5	0.23	0.985	66.0	50.05	0.982	0.088	4.26	0.872
	3.50	0.10	18.1	15.62	0.902	10.0	4.3	0.17	0.952	18.5	10.40	0.913	0.067	2.63	0.739
	3.50	0.30	27.5	15.23	0.843	21.6	0.9	0.42	0.992	28.0	48.80	0.932	0.070	3.05	0.934
	3.50	0.65	28.0	16.55	0.862	21.8	1.1	0.41	0.979	28.5	15.04	0.963	0.073	3.07	0.946
	3.50	1.00	37.0	23.08	0.845	28.2	2.1	0.36	0.986	37.5	19.80	0.975	0.075	3.35	0.965
	3.75	10.00	37.9	21.91	0.834	28.6	2.0	0.37	0.991	38.5	20.05	0.967	0.075	3.36	0.969
	3.50	30.00	65.6	30.55	0.769	35.3	4.6	0.28	0.990	50.0	33.00	0.977	0.080	3.87	0.957
	3.06	1.00	27.3	23.70	0.990	25.7	0.1	0.81	0.999	27.5	17.29	0.993	0.054	3.18	0.750
	3.03	2.00	39.5	29.62	0.970	36.1	0.5	0.56	0.976	40.5	81.88	0.991	0.053	3.54	0.817
STA	3.03	4.00	49.6	31.00	0.910	41.7	1.9	0.38	0.987	50.5	81.88	0.987	0.060	3.72	0.910
	3.03	10.00	59.7	32.00	0.900	51.1	2.9	0.32	0.979	61.0	35.68	0.991	0.050	3.95	0.908
	3.02	29.20	67.3	32.31	0.700	47.4	10.7	0.17	0.958	68.0	37.33	0.982	0.065	3.98	0.866

NOTE: JONQ = Jonquière clays; STA = St-Alban clays; S = Salinity (g/L); The yield stress and viscosity is related to Bingham model (τ_c_B, η_h), Herschel-Bulkley (τ_c_HB, n, K) and bilinear model (τ_c_bi). The Newtonian viscosity η_l (Pa.s) is determined from the initial 2 points of the bilinear model. A and B are the strength parameters in log-log diagram. Coefficient of determination R-squares (r^2) shows how well the data are explained by the best-fit line. All tests mentioned in this table are conducted using the sensor MV-II.

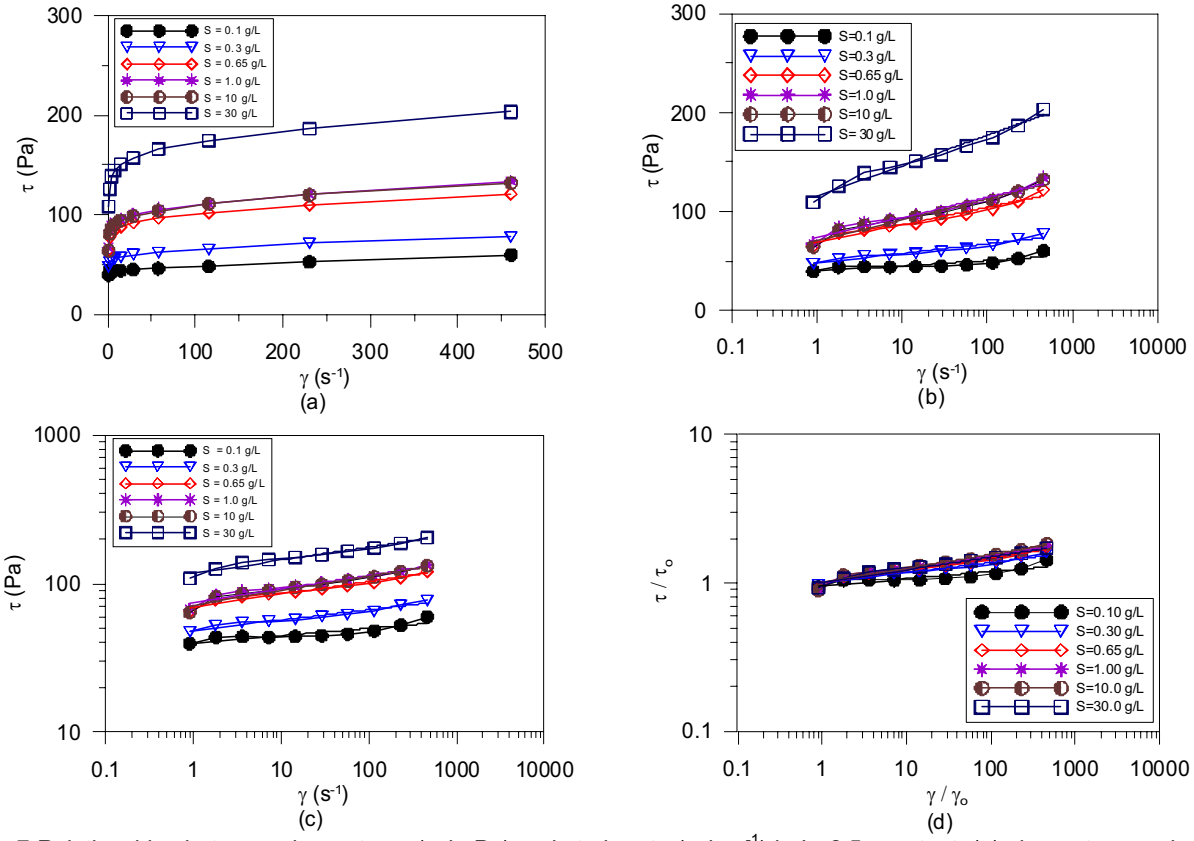

Fig. 7 Relationships between shear stress (τ, in Pa) and strain rate (γ, in s^{-1}) in I_L=2.5 constant. (a) shear stress - shear rate; (b) shear stress – log shear rate; (c) log shear stress – log shear rate; and (d) normalized log shear stress (Pa) - log strain rate (s^{-1}).

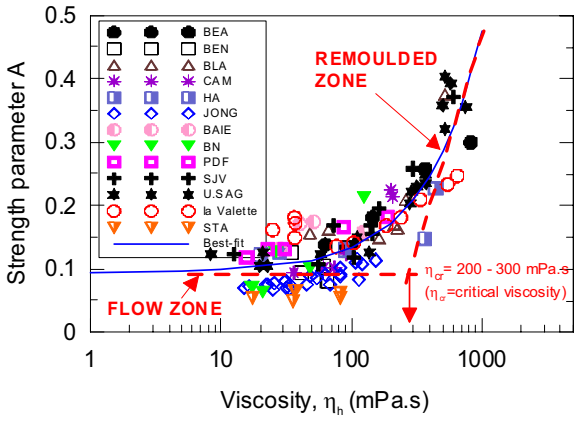

Fig. 9 The relationship between *A* and plastic viscosity at various liquidity indices

The variation of *A* values with salinities and liquidity indices is shown in Fig. 8. It appears that *A* only slightly increases with increasing salinity. On the other hand, *A* increases much more significantly when liquidity index changes (Table 3). It indicates that the water infiltration during shearing is the most important factor associated with transformation. Figure 9 shows the relationship between strength parameter *A* and plastic viscosity (η_h). It appears that the behaviour of fluid is dramatically changed as it passed from the remoulded zone (*A* = 0.3 ~ 0.4) to the flow zone (*A* = 0.05 ~ 0.15). Both of subaerial and subaqueous materials have a same pattern, even if the scatter is significant. The influence of plastic viscosity with strength parameter is varied with 1 ~ 1000 (mPa.s). In Figure 9, there seems to be an inflection point where material behaviour passes from flow-like to more flow-like characteristics. This suggests that a critical viscosity exists. The value of critical viscosity seems to be between 200 and 300 (mPa.s) for subaqueous materials.

4. DISCUSSIONS

The rheological transformations associated with submarine mass movements were examined using laboratory vane tests and viscometric data. Basically, the rheolgocial properties, *i.e.*, yield stress (τ_c) and viscosity (η), not for all but, can be linking to the liquidity index (I_L) and salt concentrations proposed by Locat and Demers (1988) and Perret et al. (1996). The previous addressed rheological models were applied for the Jonquière and St-Alban clays. Bingham, Power

law and bilinear model are well accepted in the sensitive marine clays. It should be noted, however, that the best-fit is given with a bilinear model. As for Power law, flow behavior is well defined wherever yield stress is negligible. And Bingham model is an available only at low salinity and high liquidity index.

Locat et al. (1996) described that the break-up mechanisms in the combined phenomena between increased water content and reduced shear strength to provide a flow-like behaviour. This process can explain using laboratory vane (Fig. 3). The extent of the phenomena is now well known (Locat and Lee, 2002), but there is still many unknowns. The following discussion in Fig. 10 is the most interesting part of this study associated with the rheological transformation.

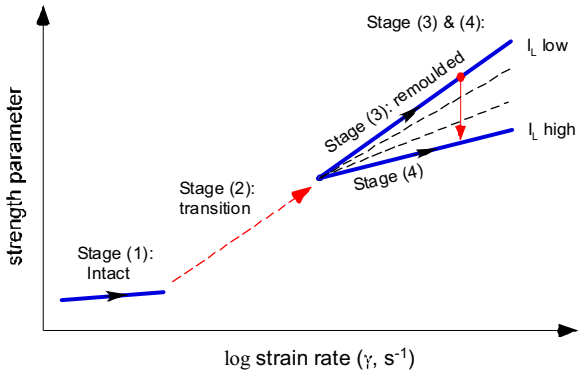

Fig. 10 Conceptual view representing the strength parameter with strain rate.

The strength parameter associated with strain rate (s^{-1}) is conceptually shown in Fig. 10. In stage (1), the variation of the strength parameter, $\Delta C_u/C_u$, is typically of 10 ~ 15% per log cycle of rate when inorganic intact clays are considered (Leroueil and Marques, 1996). From the rheological analysis using Eq. 3, the strength parameter *A* in stage (3) decreases with increasing water content or decreasing solid concentration. In stage (2), the difference between intact and remoulded stage (*i.e.*, stage 4 in Fig. 10) is significant. It may be possible if considerable water infiltration interacts with the submerged soils to rapidly reach the remoulded strength. It is also believed that it may be due to different strain rates in field and laboratory, so that the latter has a much higher value.

5. CONCLUSIONS

Based on our hypothesis, the laboratory vane tests show that the water infiltration during shearing helps to reduce the undrained shear strength. As for new log-log approach between shear stress (τ) and strain rate (γ), the normalized strength parameters *A* in all tests are shown as roughly 0.1 ~ 0.4, corresponding to about 34 % in log-log relations for all materials. It appears that *A* only slightly increases with increasing salinity. On the other hand, *A* increases much more significantly when liquidity index changes. From the relationships between the strength parameter *A* and plastic viscosity (η_h), the rheological transformation can be explained as a mechanism that increases mobility due to water infiltration during post-failure stage.

6. ACKNOWLEDGEMENTS

The authors would like to thank NSERC Canada (Natural Sciences and Engineering Research Council) via the COSTA-Canada project for providing the financial support.

7. REFERENCES

Coussot, P. 1997. Mudflow rheology and dynamics. Balkema, Rotterdam. 272p.

Imran, J., Parker, G., Locat, J. and Lee, H. 2001. 1D numerical model of muddy subaqueous and subaerial debris flows, Journal of Hydraulic Engineering, Vol. 127, No. 11: 959-968.

Leroueil, S. and Marques, M.E.S. 1996. Importance of Strain rate and Temperature effects in Geotechnical Engineering. In Measuring and Modeling Time dependent Soil Behavior, ASCE GSP 61, Sheahan, T.C. and Kaliakin, V.N. (eds.), Washington D.C., pp.1-60.

Locat, J., and Demers, D. 1988. Viscosity, yield stress, remoulded strength, and liquidity index relationships for sensitive clays. Canadian Geotechnical Journal, 25: 799-806.

Locat, J., Lee, H.J., Nelson, H.C., Schwab, W.C., and Twichell, D.C. 1996. Analysis of the mobility of far reaching debris flows on the Mississippi Fan, Gulf of Mexico. In Proceedings of the 7th International Symposium on Landslides. Edited by K. Senneset. A.A. Balkema, Rotterdam, pp. 555-560.

Locat, J. 1997. Normalized rheological behaviour of fine muds and their flow properties in a pseudoplastic regime. Proceedings 1st International conference on Debris-Flow Hazards Mitigation, San Francisco. ASCE, New York, pp. 260-269.

Locat, J. and Lee, H.J. 2002. Submarine landslides: advances and challenges, Canadian Geotechnical Journal, 39: 193-212.

Matignoni, P. and Locat, J. 1991. Évaluation de la thixotropie d'un sediment argileux par viscosimétre, Rapport GREGI 91-27. Université Laval, pp.121.

Perret, D., Locat, J., and Martignoni, P. 1996. Thixotropic behavior during shear of a fine-grained mud from Eastern Canada. Engineering Geology, 43: 31-44.